A competitive binding model predicts nonlinear responses of olfactory receptors to complex mixtures

Vijay Singh[1,2 *], Nicolle R. Murphy[3], Vijay Balasubramanian[1,2,±], Joel D. Mainland[3,4,±]

[1]*Computational Neuroscience Initiative, University of Pennsylvania, Philadelphia, PA, 19104, USA.*

[2]*Department of Physics, University of Pennsylvania, Philadelphia, PA, 19104, USA.*

[3]*Monell Chemical Senses Center, Philadelphia, PA, 19104, USA.*

[4]*Department of Neuroscience, University of Pennsylvania, Philadelphia, PA, 19104, USA.*

[*] Corresponding Author
[±]Equal contribution

Abstract: In color vision, the rules for mixing lights to make a target color are well understood. By contrast, the rules for mixing odorants to make a target odor remain elusive. The solution in vision relied on characterizing receptor responses to different wavelengths of light and subsequently relating receptor responses to perception. In olfaction, however, experimentally measuring the receptor response to a representative set of complex mixtures is intractable due to the vast number of possibilities. To meet this challenge, we develop a biophysical model that predicts mammalian receptor responses to complex mixtures using responses to single odorants. The dominant nonlinearity in our model is competitive binding: only one odorant molecule can attach to a receptor binding site at a time. This simple framework predicts receptor responses to mixtures of up to twelve monomolecular odorants to within 10-30% of experimental observations and provides a powerful method for leveraging limited experimental data.

INTRODUCTION

In the field of flavors and fragrances, methods for mixing odorants to make a target odor are largely the domain of experts who have undergone years of training. Their expertise comes from examining historical formulae as well as extensive trial-and-error work, and their methods are primarily qualitative. In vision, by contrast, the rules for mixing lights to make a target color are quantitative and well-developed. These rules are derived from a detailed characterization of human color perception and its relation to cone photoreceptor spectral sensitivities (Wandell, 1995) (Brainard & Stockman, 2010). Indeed, known tuning curves relate the wavelength of light to the responses of three types of cone photoreceptors. These input-response functions are then incorporated into models that extrapolate from the responses to single wavelengths to an arbitrary mixture of wavelengths. Finally, these receptor responses are used to predict color perception.

Here, we propose an analogous approach for characterizing the response of receptors to single odorants and modeling the responses to combinations of odorants. Simple linear models fail at this task, as a number of non-additive mixture interactions have been characterized, including suppression, masking, hyperadditivity (or synergy), hypoadditivity (or compression), configural perception, and overshadowing. The wide variety of mixture interactions suggests that a simple model would struggle to explain experimental results, but here we show that a minimal biophysical description of odorant-receptor interaction incorporating the simplest possible nonlinearity, namely competition between molecules for the binding site, can successfully predict the responses of many mammalian odor receptors to complex molecular mixtures. Previously, Rospars et al. (2008) (Rospars, Lansky, Chaput, & Duchamp-Viret, 2008) had found that responses of olfactory receptor neurons to simple binary mixtures were largely consistent with a similar model, and could display both hyper- and hypo-additivity. Cruz and Lowe (2013) (Cruz & Lowe, 2013) subsequently developed a biophysically motivated version of this model and applied it to glomerular imaging. Marasco et al. (2016) (Marasco, De Paris, & Migliore, 2016) extended this work to allow different odorants to have different Hill coefficients, and thus different degrees of binding cooperativity, which allowed for the phenomena of synergy and inhibition, although a biophysical motivation was lacking.

Here, we present three key steps forward. First, we collect receptor data for a large set of odors and show that our competitive binding model accounts for the response of olfactory receptors to complex mixtures of up to 12 odorants. Second, we develop a strategy for evading practical experimental limitations that often impede estimation of the parameters for a receptor response model. Third, our approach to biophysical modeling provides a recipe for incorporating other types of interactions among odor molecules and receptors, including consequences of having multiple binding sites, facilitation by already bound odorants, non-competitive inhibition, and heterodimerization of odorant molecules in mixture. The extended model predicts effects such as synergy, antagonism (Oka, Omura, Kataoka, & Touhara, 2004) and overshadowing (Schubert, Sandoz, Galizia, & Giurfa, 2105) in receptor responses,

phenomena that are reported in studies of human olfactory perception (Ishii, et al., 2008) and whose origin is unknown. This suggests that nonlinear effects that were previously assumed to be of neural origin may already have a strong contribution from interactions at the level of the receptor.

RESULTS

Selection of receptors that respond to multiple odorants and their mixtures

We used a heterologous assay to measure receptor responses to three monomolecular odorants (eugenol, coumarin, and acetophenone). These odorants were previously shown to be broad activators of mammalian odor receptors (Saito, Chi, Zhuang, Matsunami, & Mainland, 2009). We measured the response of 22 human and mouse olfactory receptors to these odorants and selected 18 receptors that responded at least two of the three tested odorants (Fig. 1).

A competitive binding model predicts receptor responses to mixtures

Receptor responses to odorants can be modeled in terms of the binding/unbinding of molecules to the receptor binding site. We assumed that only one molecule can attach to a binding site at a time, leading to competition. In the presence of many odorants, the outcome of competition depends on three parameters: the concentration of the individual molecules, the efficacy with which the molecule activates the receptor, and the affinity of the molecule for the binding site.

We modeled the response of a receptor to the binding of an odorant as a two-step process (see Methods). In the first step, the molecule binds reversibly to the binding site. At this stage, the bound receptor can either dissociate, giving back the odorant and the unbound receptor, or can reversibly go to an active state. The transition to the active state is the second step. In the active state, the odorant-receptor complex elicits a detectable response. In our experiments, this response is the total luminescence of luciferase reporters attached to a population of cloned receptors (Trimmer, Snyder, & Mainland, 2014).

In this competitive binding (CB) model, the response of a receptor $F(\{c_i\})$ to a mixture of N odorants with concentrations c_i is given by (derivation in SI):

$$F(\{c_i\}) = \frac{F_{max} \sum_{i=1}^{N} \left(e_i \frac{c_i}{EC50_i} \right)}{\left(1 + \sum_{i=1}^{N} \frac{c_i}{EC50_i} \right)} \qquad (1).$$

Here, $EC50_i$ is the concentration at which the response is half of the maximum for odorant i, e_i is the efficacy of the receptor for odorant i, and F_{max} parameterizes the total receptor concentration and overall response efficiency (see SI).

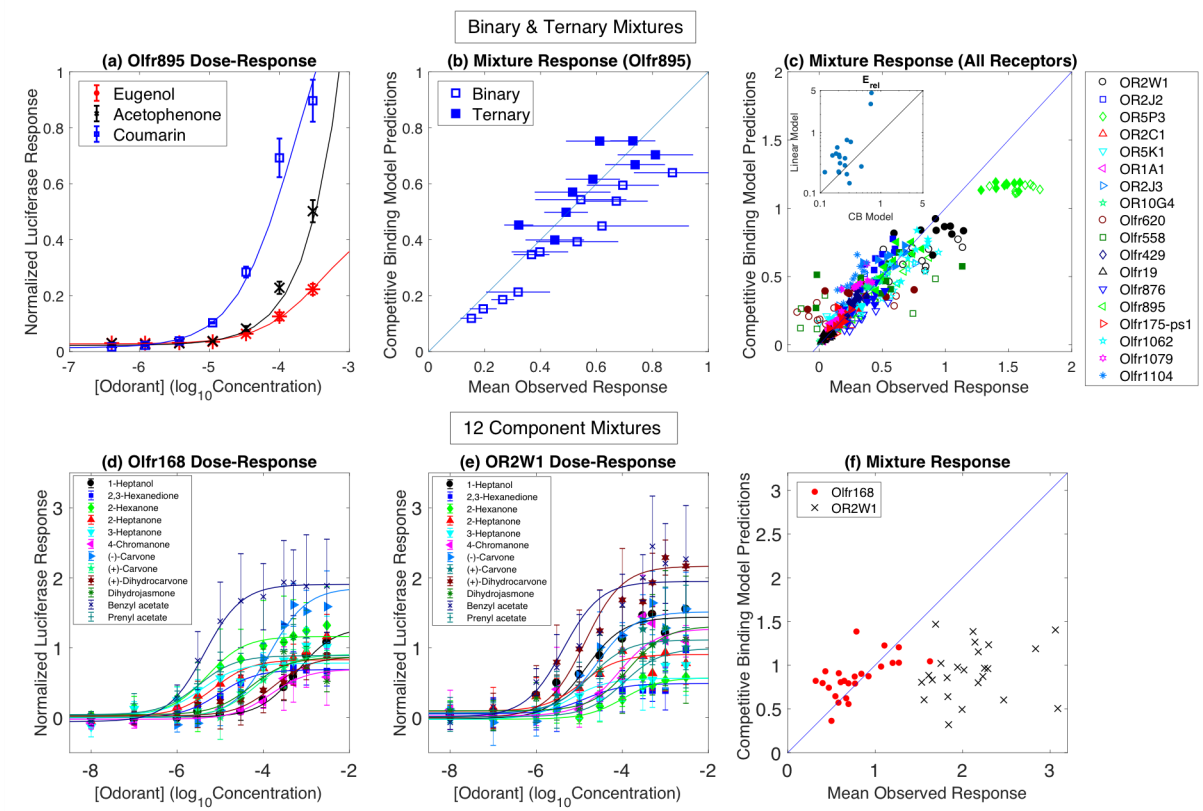

Fig 1: A competitive binding model predicts olfactory receptor response to mixtures (**a**) Response of receptor Olfr895 to individual odorants. Markers show mean experimental response +/- one standard deviation. Smooth curves show the competitive binding (CB) model with parameters chosen to minimize mean squared error between model and data (see text and Methods). (**b**) Response of Olfr895 to binary and ternary mixtures. CB model predictions are plotted against experimental responses averaged over 4 replicates. Horizontal bars represent +/- one standard deviation. (**c**) Response of 18 olfactory receptors from either humans or mice to binary and ternary mixtures (CB model vs. experimental responses averaged over four replicates)**.** For 15 of the 18 tested receptors, the relative error was between 10-33%. (**c, Inset**) The CB model has lower relative error than a linear model. (**d-e**) Response of two broadly tuned receptors, Olfr168 (mouse) and OR2W1 (human), to 12 individual odorants. (**f**) CB model predictions v/s experimental responses averaged over four replicates for Olfr168 and OR2W1 responding to 12-component mixtures**.**

The eighteen receptors previously selected were stimulated with 21 mixtures (12 binary, 9 ternary) of eugenol, coumarin and acetophenone (Methods; SI Table 1). We first fit the CB model to the dose-response data for individual odorants (N=1 in Eq. 1). We selected parameters to minimize the mean squared error between predictions and measurements (SI Table 3), weighted by the experimental standard deviation (Methods; example in Fig. 1a). The model with parameters that best reproduced the single-odorant data was then used to predict the response of the receptor to odorant mixtures (Fig.

1b,c). For most receptors (15 out of 18), the relative error (E_{rel}; see Methods) was below 33%, and in most cases well below (Fig. 1c). For the other receptors, the relative error was: 70% (Olfr620), 68% (Olfr558), and 48% (Olfr876). The competitive binding model performed significantly better than a linear model where mixture responses were predicted to be linear sums of responses to individual odorants taken from the dose-response analysis (Fig. 1c inset).

To further challenge the model, we studied the response of olfactory receptors to mixtures that were more comparable to natural odors in their complexity. We focused on two receptors, Olfr168 (mouse) and OR2W1 (human), that had broad tuning to odorants (Saito, Chi, Zhuang, Matsunami, & Mainland, 2009). From the data in (Saito, Chi, Zhuang, Matsunami, & Mainland, 2009) we identified 12 odorants that evoked responses in both receptors (Methods). Similar to the procedure above, we first fit the dose-response measurements for all 12 odorants to get the best parameters for each receptor (Fig. 1d-e) (SI Table 4). Then, we used the competitive binding model to predict receptor responses to mixtures with all 12 odorants present in diverse proportions (Methods; Fig. 1f). The model predicted the receptor responses to these complex mixtures (Olfr168: E_{rel} = 35%; OR2W1: E_{rel} = 55%), and in both cases the CB model outperformed a linear model of mixture response (Olfr168: E_{rel} = 302%; OR2W1: E_{rel} = 88%).

Improved inference of the model: dealing with unconstrained parameters

The predictive power of our model depends in part on the quality of parameters inferred from responses to single odorants. For good estimates of the parameters the experiment should capture three characteristic parts of the dose-response curve: the threshold at low concentrations, monotonic increase of response at intermediate concentrations, and saturation at high concentrations. In practice, our ability to measure response saturation of olfactory receptors was limited because cells in our preparation did not survive exposure to odorant concentrations higher than approximately 3mM. In such cases, the model parameters are not fully constrained and there are a range of parameter choices that give an equally good description of the measured responses to single odorants (Fig. 2a, SI Fig. S1). Such unconstrained directions in parameter space are common in biological experiments (Brown & Sethna, 2003) (Gutenkunst, et al., 2007), often because of the difficulties of sampling the extremes of nonlinear response functions. This limitation cannot be overcome by collecting more data at lower concentrations.

As an alternative approach, we used a subset of the mixture response data to constrain the parameters. We formed a training set of receptor responses to dose-response measurements and a subset of mixture response measurements and minimized the mean squared error (see above and Methods). We constrained the parameters to be consistent across both the dose-response measurements and the mixture measurements, and then used these parameters to predict the response to the remaining mixtures. Note that the mixtures used for training and predictions had different compositions. For example, for the 18 receptors used in binary/ternary

analysis, we used only three binary mixtures to constrain the parameters, but both binary and ternary mixtures to evaluate the model. Similarly, for the 12-component mixtures, the mixtures in the training and test sets had different compositions.

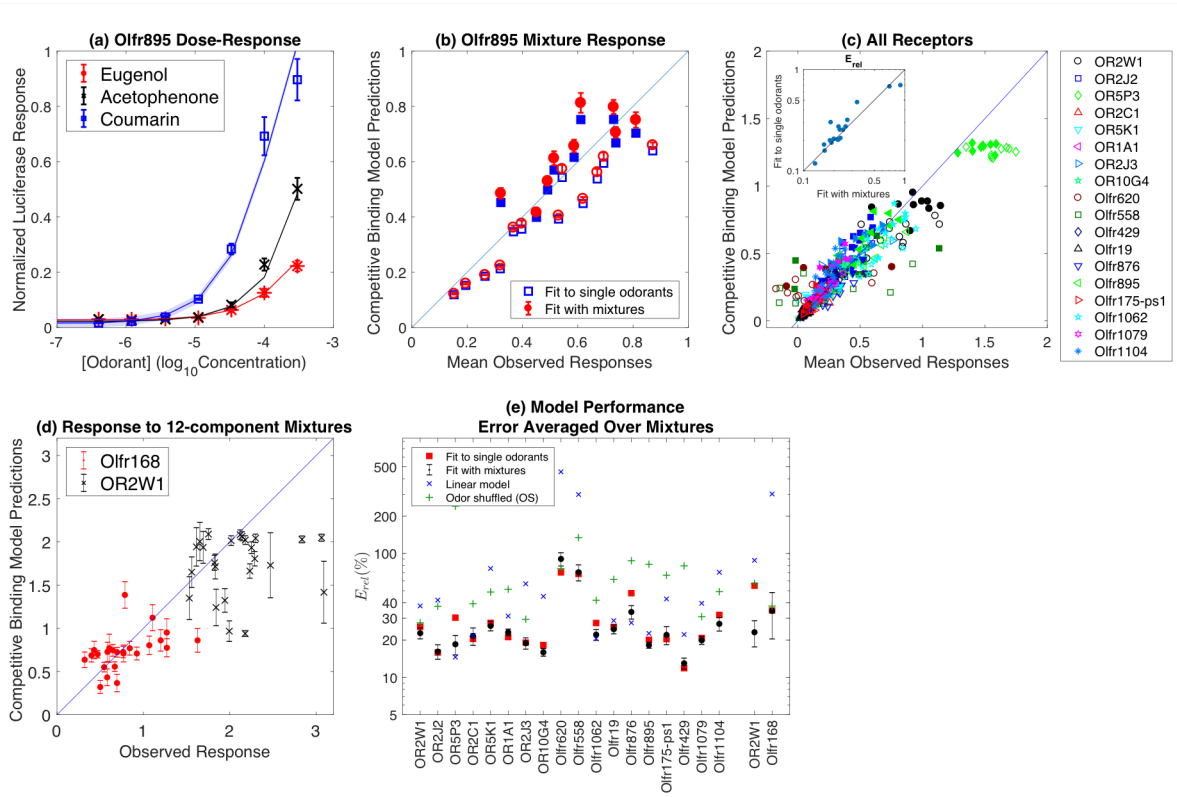

Fig 2: Model prediction improves with well constrained parameters. The parameters of the model in Fig. 1 were constrained by expanding the training set to include a small number of mixtures (see text & Methods). (**a**) Olfr895 responses fit by mixture-constrained model (solid lines). (**b**) Olfr895 responses to binary and ternary mixtures compared with model predictions (mean and standard deviation over test sets). Open markers = binary mixtures, filled markers = ternary mixtures. (**c**) Responses of 18 olfactory receptors from either humans or mice to binary and ternary mixtures (mixture-constrained CB model vs. mean observation). (**c, Inset**) Relative error for a model trained only on dose response data v/s the model trained on both dose-response and mixture data. The mixture-constrained model has lower error. (**d**) Mixture-constrained model predictions vs. experimental responses averaged over 4 replicates for Olfr168 and OR2W1 responding to 12-component mixtures**.** Error bars, s.d. over test sets. (**e**) Comparison of the relative error of mixture-constrained competitive binding model with alternative models (see text). The eighteen receptors of the binary-ternary analysis are on the left and the two receptors of the 12-component analysis are on the far right. The model with mixture-constrained parameters is the most accurate.

Including mixture data does not affect the prediction quality for responses to single odorants (Fig. 2a), but significantly improves the predictions for held out binary-ternary mixtures (Fig.2 b-c) for most receptors (Fig. 2c inset; average improvement in relative error = 11%). The relative errors for two receptors (Olfr620 and Olfr558) remains high (E_{rel} ~70%).

As discussed earlier, every dose-response curve where saturation has not been fully characterized has one unconstrained parameter. For our mixtures with 12 components, this limitation led effectively to 12 free parameters. To constrain these, we needed to expand the model training set to include mixture data. We selected a training set size of 12 mixtures. Thus, we had equal number of mixtures in our training and test sets. We assigned the mixtures chosen for the training and test sets randomly and calculated the relative error over 300 such assignments. The relative error averaged over assignments was 35% for Olfr168 and 24% for OR2W1, a significant improvement (compare Fig. 2d and Fig. 1f).

A competitive binding model outperforms a linear model

We compared the results of our model to a linear model where the mixture response is a linear sum of the receptor responses to individual odorants at their concentration in the mixture. In addition, we tested our model on a shuffled dataset where instead of using the dose-response curves of the mixture components, we selected random dose-response curves from the set of odors tested on a given receptor (odor shuffled). This comparison tests whether the specificity of receptor-odorant interactions determines the model accuracy, or whether good prediction results from simply fixing responses to be sigmoidal in the right range for each receptor separately (Methods).

For binary and ternary mixtures, the competitive binding model (with parameters constrained by a limited amount of mixture data) outperformed both alternatives models (Fig. 2e). Similarly, for 12-component odors, the relative error of the mixture-constrained CB model (Olfr168 35%, OR2W1 22%) was much lower than the error of the alternative models (Olfr168: linear 302%, OS 40%; OR2W: linear 88%, OS 57%).

Extensions of the model

So far, we have considered the simplest possible form of odorant-receptor interaction: only one odorant molecule binds a receptor binding site at a time. Surprisingly, most of the receptors studied in our experiments were well-described by this model. Competitive binding can produce essentially three types of nonlinear receptor response to presentation of mixtures (Fig. 3a-e): (1) Domination by the odorant that gives the highest response individually (*overshadowing*, Fig. 3a-b), (2) A response in between those to the individual odorants (*suppression*, Fig. 3c), (3) Domination by the odorant that gives the lowest individual response (also called *overshadowing*, Fig. 3d-e). These effects can arise both from the intrinsic properties of the receptor-odorant

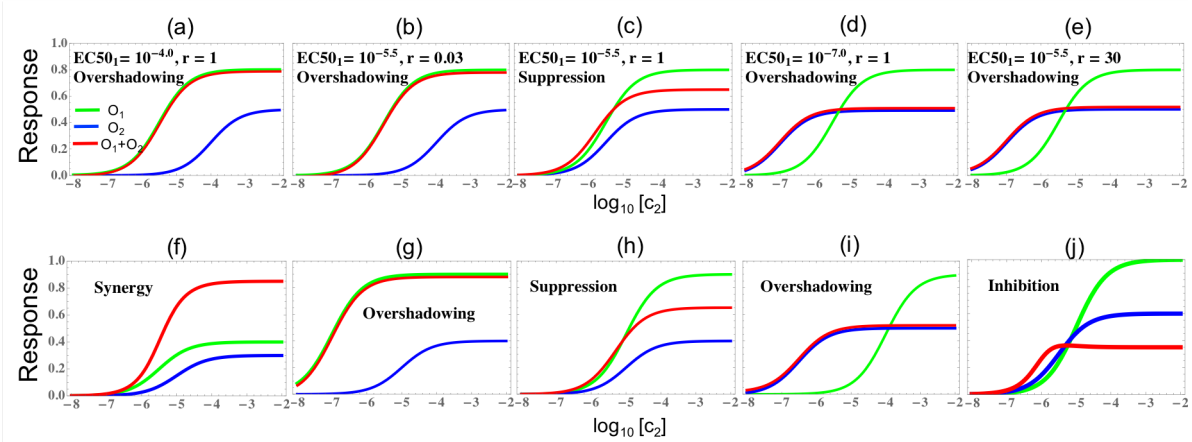

Figure 3: (Top Row): Phenomena exhibited by the competitive binding model. The competitive binding model with different parameter choices shows diverse effects for binary mixtures (purple) of two odorants (red and blue). Shown here are effects due to variations of $EC50_1$ and of the ratio of odorant concentrations in mixture $r = c_1/c_2$: (**a-b**) overshadowing by the odorant with the higher individual response, (**c**) suppression, where the response is in between the responses of the individual odorants and (**d-e**) overshadowing by the receptor that produces the lower individual response. Value of the other model parameters: $F_{max} = 1, e_1 = 0.5,\ e_2 = 0.8$ and $EC50_2 = 10^{-5.5}$. **(Bottom Row): Phenomena exhibited by the extended model including odorant facilitation**. Facilitation of odorant binding by another odorant molecule in mixture leads to additional effects like synergy and inhibition. (**f**) Synergy: receptor response is higher than response to both the individual odorants. (**g**) Overshadowing by the more reactive odor, (**h**) Suppression, (**i**) Overshadowing by the less reactive odor, (**j**) inhibition, where response to mixtures is lower than the response to either individual odorant.

interaction (difference in EC50, Fig. 3a,c,d) or due to extrinsic factors such as the ratio of the concentrations (Fig. 3b,c,e). Such qualitative effects have been reported previously (Marasco, De Paris, & Migliore, 2016) in a phenomenological model that has a more complex form of response to mixtures. We have shown here that these effects can already be exhibited by a simple model directly rooted in biophysical competition between the odorant molecules seeking to occupy the receptor.

Our model can be easily extended to incorporate additional biophysical interactions that produce effects such as synergy (Ishii, et al., 2008) and inhibition (Sanhueza, Schmachtenberg, & Bacigalupo, 2000). Although previous work (Rospars, Lansky, Chaput, & Duchamp-Viret, 2008) (Marasco, De Paris, & Migliore, 2016) (Cruz & Lowe, 2013) has explored possible mathematical functions that can be used to fit such nonlinearities in receptor response data, a biophysical understanding of the origins of these effects has been missing. Some recent progress on this front is reported in (Reddy, Zak, Vergassola, & Murthy, 2018). Our approach of starting from the simplest interactions at the molecular level provides a potential avenue for further progress. For example, the minimal competitive binding model can be readily extended to include

more complex interactions. For example, consider *facilitation*, where the binding of an odorant promotes the binding of other odorants to the same site. This interaction leads to a modification in Eq. 1 (see SI) and produces diverse effects such as synergy (Fig. 3f), in which the response of the receptor is higher than the sum of the response to both individual odors, overshadowing (Fig.3g, i), suppression (Fig. 3h), and inhibition (Fig. 3i) where the response is below the response of both individual odorants. Alternatively, if there are multiple independent binding sites for odorants, the mixture response will be the sum of the individual components (SI). More complex biophysical interactions, such as non-competitive inhibition (SI), hetero-dimerization (SI), catalysis by odor molecules, etc. can similarly be added to the basic model in a principled way.

DISCUSSION

In this work, we showed that a minimal biophysical model of odorant-receptor interaction incorporating just the simplest possible nonlinearity, namely competition between molecules for the binding site, can successfully predict the responses of many mammalian odor receptors to complex molecular mixtures. This was surprising because non-competitive interactions are common in pharmacology, but we nevertheless found that our simple model explains the majority of the experimental results. More general interactions between odorants and receptors can be easily added to our model, at the cost of additional parameters. For example, we showed that the nonlinearities implied by just competitive exclusion and facilitation are sufficient to produce diverse effects that have been previously reported in the perception of odor mixtures including synergy (Ishii, et al., 2008), overshadowing (Schubert, Sandoz, Galizia, & Giurfa, 2105), suppression (Simon & Derby, 1995) and inhibition (Sanhueza, Schmachtenberg, & Bacigalupo, 2000). These effects were thought to have a neural origin, but our results suggest that they may in fact be driven partly by the biophysics of receptors.

Experimental studies of olfaction have largely focused on simple odors consisting of only one or two odorant molecules. However, natural odors are generally complex, containing hundreds of volatile components, with 3-40 being essential for the characteristic odor (Dunkel, et al., 2014). Thus, in order to understand how olfactory circuits operate in naturalistic environments, models must account for complex sensory stimuli, as visual neuroscience has done for some time. A first step towards this goal is to understand how the receptors themselves respond to mixtures of many molecules. In practical terms, the combinatorial explosion of the number of mixtures with different compositions means that the only hope for progress is to have a model that can predict mixture responses from dose-response curves, which can conceivably be measured for large panels of odorants in high throughput experiments. Such a predictive model is most likely to be successful if it is rooted in the basic biophysics and biochemistry of molecular sensing, as our model is.

Estimating the parameters of our model was challenging for some receptors because of constraints on the experimental design. Complex biological systems are often difficult to fully probe experimentally, leaving unconstrained parameters even when there is apparently enough data (Brown & Sethna, 2003) (Gutenkunst, et al.,

2007). In this situation, the key is to identify measurements that indirectly constrain the parameters when a direct measurement is not possible. In our case, for example, a key challenge was that many receptors saturate at odor concentrations that would kill the cells, so we could only measure the low concentration portion of the individual dose-response curves. As a result, some parameters in our model were unconstrained. Additional measurements of response at low individual concentrations would not impose new constraints on the parameters. However, we found an indirect method of effectively constraining the parameters: using multiple odors, each at a low concentration, to stimulate the receptor simultaneously. These measurements allow only those parameter values that are consistent both with individual responses and mixture responses. Thus, after measuring the response to individual odorants at a few concentrations, it is more informative to measure response to a few small mixtures. A lesson for the future is that experiments should be designed to appropriately probe the different directions of the parameter space of complex, nonlinear models.

In olfaction, the low background activity of most receptors also makes it difficult to identify inverse agonists or antagonists using single molecules. But these effects, and more general non-competitive interactions, do occur in mixtures. Fortunately, such interactions will typically involve small numbers of molecules as the probability of multiple molecules meeting to interact at the same time should decline exponentially with the number of interacting molecules. Thus, future studies should be able to explore the landscape of interactions by testing receptor responses to mixtures with just a small number of components.

In the study of color vision, models of the early visual system are combined with look up tables of human responses to primary colors obtained through psychophysical experiments (CIE, 1986) to predict responses to arbitrary colors. These models have led to accepted industry standards that are used to produce color graphics through electronic or print means. Perhaps lookup tables of dose-response curves for olfactory receptors could be combined with models such as ours to predict responses to complex mixtures, ultimately allowing olfactory designers to create desired odors from a set of primary odorants.

Author Contributions

Concept and design: VS, NM, JM, VB. Performed experiments: NM, JM. Model and analysis: VS, VB.

Acknowledgements

VB and VS were supported by the Simons Foundation (Grant 400425; Mathematical Modeling of Living Systems). Work by VB at the Aspen Center for Physics was supported by NSF grant PHY-1607611. NM and JM were supported by R01 DC013339. A portion of the work was performed using the Monell Chemosensory Receptor Signaling Core and Genotyping and DNA/RNA Analysis Core, which was supported, in part, by funding from the US National Institutes of Health NIDCD Core Grant P30 DC011735.

METHOD DETAILS

Cell-based assay

In vitro experiments followed the protocol for a Dual-Glo Luciferase Assay System (Promega) described in (Zhuang & Matsunami, 2008) (Trimmer, Snyder, & Mainland, 2014). Hana3A cells (curtesy of Matsunami Laboratory), were plated into 96-well poly-D-lysine-coated plates (Corning BioCoat). Negative mycoplasma status and cell line identity were confirmed for cells used in these experiments (ATCC; Promega). Plated cells were transfected with 5 ng/well of RTP1S-pCI (Saito, Kubota, Roberts, Chi, & Matsunami, 2004) (Zhuang & Matsunami, 2008), 5ng/well of pSV40-RL, 10ng/well pCRE-luc, 2.5 ng/well of M3-R-pCI (Li & Matsunami, 2011), and 5 ng/well of plasmids containing rhodopsin-tagged olfactory receptors. Each plate was transfected with eight wells of Olfr544 as a standard. Twenty-four hours after transfection, we applied each monomolecular odorant or mixture in quadruplicate. Odors were diluted to the final concentration in CD293 (ThermoFisher Scientific). To standardize across plates, half of the standard wells were stimulated with CD293 (no odor) and half were stimulated with 100uM Nonanedioic acid (Sigma-Aldrich) in CD293. All olfactory receptors on a given plate were stimulated with the same odorant or mixture. Four hours after odor stimulation, we measured luminescence according to the Dual-Glo protocol (BioTek Synergy 2 reader).

Binary and Ternary Mixtures

Based on data from (Mainland, Snyder, & Botero, 2013), we identified 22 receptors likely to respond to Eugenol, Acetophenone, and Coumarin (Sigma-Aldrich). We applied seven steps of three-fold serial dilutions for each odorant starting at 300uM as well as a no-odor control. Odors were applied in quadruplicate to all 22 receptors to obtain dose response curves for each receptor. Four receptors, Olfr362, Olfr315, Olfr1110, Olfr165, were not tested with subsequent mixtures because they did not respond to at least two of the three odorants. For the 18 remaining receptors, we measured the responses to twelve binary and nine ternary mixtures of Eugenol, Acetophenone, and Coumarin (see Supplementary Table 1 for mixture compositions).

12-Component Mixtures

From previously collected measurements of olfactory receptor responses to monomolecular odorants (Saito, Chi, Zhuang, Matsunami, & Mainland, 2009) we identified eight receptors that are broadly tuned. Two of the eight had complete dose-response curves for more than 12 odors (Olfr168 responded to 37 odorants and OR2W1 to 23 odorants (Saito, Chi, Zhuang, Matsunami, & Mainland, 2009)). We identified 17 odorants that activated both receptors in this data. We chose the twelve odorants with the lowest EC50s for further experiments (list in Fig 1d, inset) and used the dose response data from (Saito, Chi, Zhuang, Matsunami, & Mainland, 2009) to estimate model parameters. We tested 24 mixtures of 12 odorants as well as a no-odor control. Six of the mixtures contained all 12 odorants at equimolar concentrations. For the other 18 mixtures, we used the model to select pseudo-random concentrations of

each odorant such that the predicted receptor response spanned the full dynamic range and avoided saturation (see Supp. Table 2 for the mixture compositions).

Odorants
Odorants (Sigma-Aldrich; See SI Table 5) were diluted to the final concentration in CD293 (ThermoFisher Scientific) with the exception of four odorants (4-Chromanone, Acetophenone, Coumarin, and Eugenol) that were diluted from 1M stocks in DMSO. All mixtures containing odorants diluted from 1M stocks in DMSO had less than 0.05% DMSO in the final mixture.

QUANTIFICATION AND STATISTICAL ANALYSIS

Preprocessing
We divided the Firefly luciferase luminescence by Renilla luciferase luminescence to normalize for transfection efficiency and cell death. In our system, Firefly is a measure of receptor activity while Renilla is made regardless of the receptor activity and is a measure of the response capacity, i.e., how many cells are alive and successfully transfected. Thus, we are normalizing the response capacity of the cells in the specific assay. Additionally, we divided by the difference between the standard Olfr544 response at 0uM and 100uM Nonanedioic acid. This preprocessing allowed us to compare receptor responses relative to our standard receptor and to normalize responses across plates. Lastly, we subtracted receptor response at zero concentration of odorant/mixture to get the net response above baseline.

Alternative models for comparison
1. Linear Model: The receptor response in the linear model is given by

$$F_{linear}(\{c_i\}) = \sum_{i=1}^{N} \frac{F_{max}\left(e_i \frac{c_i}{EC50_i}\right)}{\left(1 + \frac{c_i}{EC50_i}\right)}$$

where c_i are the concentrations of odorants.

2. Odor Shuffled: The odor shuffled model has the same mathematical form as Eq.1, but parameters are shuffled among the dose-response sets available for the particular receptor. For example, in the binary-ternary analysis we have three sets of dose-response parameters (corresponding to the three odorants) for every receptor. We shuffle these parameters independently among each other. Since there are six possible permutations of the EC50s and six for the product $F_{max}e_i$, we have a total of 36 shuffled sets of parameters for the odor shuffled model. The relative error was calculated over the 35 sets left after removing the original set. For the 12-component mixture, we chose 100 such randomly shuffled parameter sets for estimating the relative error.

Model parameter estimation using dose-response measurements
First, we used the response (y_{ex}) of each receptor to odorants at M concentrations. ($M = 8$ for binary-ternary analysis, $M = 11$ for 12-component mixture analysis.) to calculate the average ($\bar{y}_{ex}(c_i)$) and standard deviation ($\sigma(c_i)$) of the receptor response

to odorant i over four replicates for each concentration c_i . For each odorant, we chose parameters ($EC50_i$ and the product $F_{max}e_i$) to minimize the mean squared error between this average measured response and the model prediction $\left(F(c_j)\right)$, weighted by the experimental standard deviation, i.e.:

$$E_i = \sqrt{\frac{1}{M}\sum_{c_i}\left(\frac{F(c_i) - \bar{y}_{ex}(c_i)}{\sigma(c_i)}\right)^2}$$

$E_i = 1$ would mean that, on average, the model predictions lie one standard deviation away from the mean experimental observation. As E_i is a function of the $EC50_i$ and the products $F_{max}e_i$, we choose these parameter combinations to minimize E_i.

Parameter estimation using both dose-response and mixture response

As discussed in Results, if the saturation of the receptors cannot be determined in the dose-response experiments, the parameters obtained by minimizing the relative squared error are not well constrained. In such cases, we used receptor responses to a few mixtures to further constrain the parameters. For this purpose, we separated the mixture responses into training and test sets, and estimated parameters by combining the relative squared error for the odorant dose-response and mixture training set response as:

$$\sqrt{\frac{1}{N_o}\sum_{i=1}^{N_o} E_i^2 + \frac{1}{N}\sum_{k=1}^{N}\left(\frac{F(m_k) - \bar{y}_{ex}(m_k)}{\sigma_{m_k}}\right)^2}$$

The first term under the square root is the mean of the squared error, weighted by the standard deviation, of all dose-response measurements, with N_o being the total number of odorants for which the dose-response was measured ($N_o = 3$ for the binary/ternary experiments and $N_o = 12$ for 12-component experiments). The second term under the square root is the squared error, weighted by the standard deviation, for the mixture measurements in the training set. Here, $F(m_k)$ is the receptor response to mixture m_k, and $\bar{y}_{ex}(m_k)$ and σ_{m_k} are the corresponding experimentally observed mean response and standard deviation calculated over 4 replicates of the mixture. N is the number of mixtures in the training set. For the binary-ternary analysis, the mixture training set had *N=3*, the minimum number of data points required to constrain three dose-response curves. For a fair comparison with the model trained only on dose-response data, we removed three measurements from the dose-response data, one for each odorant. For the 12-component experiments, we used a training set of 12 mixtures. An equal number of measurements were removed from the dose-response data.

Quantifying Model Performance

We quantified the performance of the model in terms of the relative error defined as:

$$E_{rel} = \frac{1}{N_m}\sum_{i=1}^{N_m}\left(\frac{|F_i - y_i|}{y_i}\right),$$

where N_m is the number of mixtures in the test set for the experiment, F_i is the model prediction for a mixture in the test set, and y_i is the corresponding mean experimental observation. The test set consisted of all mixtures that were not included in the training set. For the binary-ternary analysis we needed three mixtures in the training set (see above), and selected one from each odorant pair: eugenol-acetophenone, acetophenone-coumarin and eugenol-coumarin. For each of these pairs there were four mixture proportions to choose from in our data. Thus, we had a total of 64 (4x4x4) unique ways of choosing the training set. The remaining test set had 18 mixtures (9 binary, 9 ternary). We report relative error (E_{rel}) as the average over all these 64 choices of training set. For the 12-component analysis we needed twelve mixtures in the training set (see above). Thus, we randomly chose 12 out of the 24 mixtures in our data as the training set, and calculated the average relative error (E_{rel}) for the remaining test set over 300 such random assignments.

Data and Software Availability

Data and software are available upon request from the authors.

Bibliography

Brainard, D., & Stockman, A. (2010). Colorimetry. In M. e. Bass (Ed.), *OSA Handbook of Optics* (Vol. 3, pp. 10.1-10.56). McGraw-Hill, New York.

Brown, K. S., & Sethna, J. P. (2003). Statistical mechanical approaches to models with many poorly known parameters. *Physical Review E, 68*(2), 021904-1-9.

CIE. (1986). Colorimetry (Report No. 15.2). *Bureau Central de la CIE*.

Cruz, G., & Lowe, G. (2013). Neural coding of binary mixtures in a structurally related odorant pair. *Scientific Reports, 3*, 1220 .

Dunkel, A., Steinhaus, M., Kotthoff, M., Nowak, B., Krautwurst, D., Schieberle, P., & Hofmann, T. (2014). Nature's chemical signatures in human olfaction: a foodborne perspective for future biotechnology. *Angewandte Chemie International Edition, 53*(28), 7124--7143.

Gutenkunst, R. N., Waterfall, J. J., Casey, F. P., Brown, K. S., Myers, C. R., & Sethna, J. P. (2007). Universally sloppy parameter sensitivities in systems biology models. *PLoS Comput Biol, 3*(10), e189.

Ishii, A., Roudnitzky, N., Beno, N., Bensafi, M., Hummel, T., Rouby, C., & Thomas-Danguin, T. (2008). Synergy and masking in odor mixtures: an electrophysiological study of orthonasal vs. retronasal perception. *Chemical Senses, 33*(6), 553-561.

Li, Y. R., & Matsunami, H. (2011). Activation state of the M3 muscarinic acetylcholine receptor modulates mammalian odorant receptor signaling. *Science Signalling, 4*(155), ra1.

Mainland, J., Snyder, L., & Botero, S. (2013). *Mammalian odorant receptor responses to mixtures of three monomolecular odorants.* Retrieved from 10.13140/2.1.3449.4409

Marasco, A., De Paris, A., & Migliore, M. (2016). Predicting the response of olfactory sensory neurons to odor mixtures from single odor response. *Scientific reports, 6*.

Oka, Y., Omura, M., Kataoka, H., & Touhara, K. (2004). Olfactory receptor antagonism between odorants. *The EMBO Journal, 23*(1), 120-126.

Reddy, G., Zak, J. D., Vergassola, M., & Murthy, V. N. (2018). Antagonism in olfactory receptor neurons and its implications for the perception of odor mixtures. *eLife*, e34958.

Rospars, J.-P., Lansky, P., Chaput, M., & Duchamp-Viret, P. (2008). Competitive and noncompetitive odorant interactions in the early neural coding of odorant mixtures. *Journal of Neuroscience, 28*(10), 2659-2666.

Saito, H., Chi, Q., Zhuang, H., Matsunami, H., & Mainland, J. D. (2009). Odor coding by a Mammalian receptor repertoire. *Science Signaling, 2*(60).

Saito, H., Kubota, M., Roberts, R. W., Chi, Q., & Matsunami, H. (2004). RTP family members induce functional expression of mammalian odorant receptors. *Cell, 119*(5), 679-691.

Sanhueza, M., Schmachtenberg, O., & Bacigalupo, J. (2000). Excitation, inhibition, and suppression by odors in isolated toad and rat olfactory receptor neurons. *American journal of physiology, 279*(1), C31-C39.

Schubert, M., Sandoz, J.-C., Galizia, G., & Giurfa, M. (2105). Odourant dominance in olfactory mixture processing: what makes a strong odourant? *Proceedings of the Royal Society of London B: Biological Sciences, 282*(1802), 20142562.

Simon, T. W., & Derby, C. D. (1995). Mixture suppression without inhibition for binary mixtures from whole cell patch clamp studies of in situ olfactory receptor neurons of the spiny lobster. *Brain Research, 678*(1-2), 213-224.

Trimmer, C., Snyder, L. L., & Mainland, J. D. (2014). High-throughput Analysis of Mammalian Olfactory Receptors: Measurement of Receptor Activation via Luciferase Activity. *Journal of visualized experiments: JoVE*(88).

Wandell, B. A. (1995). *Foundations of vision.* Sunderland, MA: Sinauer.

Zhuang, H., & Matsunami, H. (2008). Evaluating cell-surface expression and measuring activation of mammalian odorant receptors in heterologous cells. *Nature protocols, 3*(9), 1402.

Supplementary Information

1. Competitive binding model

Consider a receptor (R) interacting with a mixture of two odorants (O_1 and O_2) with concentrations c_1 and c_2, and binding affinities k_1 and k_2 respectively. Assume that only one odorant molecule can bind a receptor at a time. Upon binding, an odorant forms a receptor-odor complex O_iR, ($i = 1,2$). The complex can either dissociate with rate r_i, giving back the receptor and the odorant molecule, or can enter an active state O_iR^*, which elicits a detectable response, with rate $k_i{}^*$.

In our experimental assay, not every odorant binding event would lead to luminescence. The active state receptor represents those receptors that produce luminescence. In real systems, these are the receptors that result in a downstream response after binding to an odorant.

The complex in the active state can revert back to the inactive state with rate $r_i{}^*$. The total response is proportional to the total number of receptor-odor complexes in the active state. These interactions can be summarized by the following chemical reactions:

$$O_1 + R \underset{r_1}{\overset{k_1}{\rightleftharpoons}} O_1R \underset{r_1{}^*}{\overset{k_1{}^*}{\rightleftharpoons}} O_1R^*$$

$$O_2 + R \underset{r_2}{\overset{k_2}{\rightleftharpoons}} O_2R \underset{r_2{}^*}{\overset{k_2{}^*}{\rightleftharpoons}} O_2R^*$$

These reactions are described by the differential equations

$$\frac{dR}{dt} = -(k_1c_1\,R + \,k_2c_2\,R) + \,(r_1R_1 + \,r_2R_2)$$

$$\frac{dR_i}{dt} = (k_ic_i\,R + \,r_i{}^*\,R_i{}^*) - (r_iR_i + \,k_i{}^*R_i)$$

$$\frac{dR_i{}^*}{dt} = k_i{}^*R_i - \,r_i{}^*R_i{}^*$$

where $i = 1, 2$, with R, R_i, $R_i{}^*$ being the concentrations of receptors that are unbound, bound to odorant i but inactive, and bound in an active state to odorant i, respectively. The sum of all these concentrations is fixed to be R_{max} reflecting the total number of available receptors. Assuming that the response is proportional to the total number of bound receptors in the active state ($R^* = R_1{}^*+R_2{}^*$) we solve the rate equations at steady state to find that

$$F(\{c_1, c_2\}) = \frac{F_{max}\left(e_1\frac{c_1}{EC50_1} + e_2\frac{c_2}{EC50_2}\right)}{\left(1 + \frac{c_1}{EC50_1} + \frac{c_2}{EC50_2}\right)}$$

where $EC50_i = r_ir_i{}^*/(\,k_i(k_i{}^* + r_i{}^*))$ is the concentration at which the response is half of the maximum for odorant i, $e_i = k_i{}^*/(k_i{}^* + r_i{}^*)$ is the efficacy of the receptor for the odorant i, and F_{max} is a parameter that depends on the total receptor concentration. Fig. 3 shows the response of a receptor according to this model. For an *N* component mixture with odorant concentrations $\{c_i : i = [1, N]\}$, this result generalizes to:

$$F(\{c_i\}) = \frac{F_{max} \sum_{i=1}^{N} \left(e_i \frac{c_i}{EC50_i} \right)}{\left(1 + \sum_{i=1}^{N} \frac{c_i}{EC50_i} \right)}$$

2. Extension of the competitive binding model:

2.1 Facilitation:

It is possible that the binding of one odorant facilitates the binding of other odorants. In a mixture, such interactions can be considered through the following the chemical reaction:

$$O_1 + R \underset{r_1}{\overset{k_1}{\rightleftharpoons}} O_1R \underset{r_1^*}{\overset{k_1^*}{\rightleftharpoons}} O_1R^*$$

$$O_2 + R \underset{r_2}{\overset{k_2}{\rightleftharpoons}} O_2R \underset{r_2^*}{\overset{k_2^*}{\rightleftharpoons}} O_2R^*$$

$$O_1R + O_2 \underset{r_{12}}{\overset{k_{12}}{\rightleftharpoons}} O_1O_2R \underset{r_{12}^*}{\overset{k_{12}^*}{\rightleftharpoons}} O_1O_2R^*$$

The solution of the corresponding rate equations at steady state is

$$F(\{c_1, c_2\}) = \frac{F_{max} \left(e_1 \frac{c_1}{EC50_1} + e_2 \frac{c_2}{EC50_2} + e_{12} \frac{c_1 c_2}{EC50_{112}} \right)}{\left(1 + \frac{c_1}{EC50_1} + \frac{c_2}{EC50_2} + \frac{c_1 c_2}{EC50_{112}} \right)}$$

where $EC50_i = r_i r_i^* / (k_i (k_i^* + r_i^*))$, $e_i = k_i^* / (k_i^* + r_i^*)$, $EC50_{112} = r_1 r_{12} r_{12}^* / (k_1 k_{12} (k_{12}^* + r_{12}^*))$ and $e_{12} = k_{12}^* / (k_{12}^* + r_{12}^*)$. This simple modification with different parameters sets p={$EC50_1$, e_1, $EC50_2$, e_2, $EC50_{112}$, e_{12}, r} can account for behaviors like synergy (Fig. 3f; p={$10^{-5.5}$,0.6,10^{-5},0.4,10^{-11},0.85,1}) in which the receptor response to mixture is higher than all constituent odorants, overshadowing (Fig. 3g; p={10^{-7},0.9,10^{-5},0.4,10^{-3},0.3,1}) where the mixture response is dominated by the odorant with highest individual response, suppression (Fig. 3h; p={ 10^{-5},0.9,10^{-5},0.4,10^{-3},0.5,1}) where the mixture response is in between the individual response of the odorants, overshadowing (Fig. 3i; p=10^{-4},0.9,$10^{-6.5}$,0.5,10^{-3},0.3,1}) where the mixture response is dominated by the odorant with lowest individual response, and inhibition (Fig. 3j; p={10^{-5},0.1,$10^{-5.5}$,0.6,10^{-12},0.35,1}) in which the response is lower than the responses to all individual odorants.

2.2 Independent binding sites:

If there are independent binding sites on the receptor molecule for different odorants, then the receptor response to the mixture would simply be the sum of the response of individual odorants. For a binary mixture, the response would be given as:

$$F(\{c_1, c_2\}) = \frac{F_{max}\left(e_1 \frac{c_1}{EC50_1}\right)}{\left(1 + \frac{c_1}{EC50_1}\right)} + \frac{F_{max}\left(e_2 \frac{c_2}{EC50_2}\right)}{\left(1 + \frac{c_2}{EC50_2}\right)}$$

2.3 Non-competitive Inhibition

If the odorants bind independently to two binding sites, but the receptor responds when only the first site binding site is occupied, we can have the following set of reactions:

$$O_1 + R \underset{r_1}{\overset{k_1}{\rightleftharpoons}} O_1R \underset{r_1^*}{\overset{k_1^*}{\rightleftharpoons}} O_1R^*$$

$$O_2 + R \underset{r_2}{\overset{k_2}{\rightleftharpoons}} O_2R$$

$$O_1 + O_2R \underset{r_1}{\overset{k_1}{\rightleftharpoons}} O_1O_2R$$

$$O_2 + O_1R \underset{r_2}{\overset{k_2}{\rightleftharpoons}} O_1O_2R$$

These set of equations allows for 5 possible states of the receptor. Unbound (R), bound with odorant 1 or 2 (O_1R, O_2R), bound with both odorants (O_1O_2R) and in the bound excited state (O_1R^*). The receptor response is proportional to the concentration of O_1R^* and is given by:

$$F(\{c_1, c_2\}) = \frac{F_{max}\left(e_1 \frac{c_1}{EC50_1}\right)}{\left(1 + \frac{c_1}{EC50_1} + K_2c_2(1 + K_1c_1)\right)}$$

where $K_i^* = \frac{k_i}{r_i}$. Such interactions lead to suppression and inhibition.

2.4 Independent binding sites with facilitation:

The binding of one odorant on a receptor binding site may facilitate the binding of the other odorant on the second binding site. Such an interaction leads to the following chemical reactions:

$$O_1 + R_1 \underset{r_1}{\overset{k_1}{\rightleftharpoons}} O_1R \underset{r_1^*}{\overset{k_1^*}{\rightleftharpoons}} O_1R^*$$

$$O_2 + R_2 \underset{r_2}{\overset{k_2}{\rightleftharpoons}} O_2R \underset{r_2^*}{\overset{k_2^*}{\rightleftharpoons}} O_2R^*$$

$$O_1 + R_1 \underset{r_1}{\overset{k_{12}[O_2R]}{\rightleftharpoons}} O_1R \underset{r_1^*}{\overset{k_1^*}{\rightleftharpoons}} O_1R^*$$

These equations can be solved as earlier under the constraints ($R_1 + O_1R + O_1R^* = F_{max}$) and ($R_2 + O_2R + O_2R^* = F_{max}$). The receptor response is given as:

$$F(\{c_1, c_2\}) = \frac{F_{max}}{\left(\frac{1}{e_1} + \frac{\left(1 + \frac{c_2}{EC50_2}\right)}{e_1 \frac{c_1}{EC50_1}(1 + e_2 \frac{c_2}{EC50_2}(\frac{F_{max} k_{12} r_2^*}{k_1 k_2^*} + \frac{1}{e_2}))}\right)} + \frac{F_{max}\left(e_2 \frac{c_2}{EC50_2}\right)}{\left(1 + \frac{c_2}{EC50_2}\right)}$$

This interaction results in synergy and overshadowing by more reactive odor.

2.5 Odorant dimerization:

To include cases where different odorant molecules combine to form a heterodimer (O_1O_2) before binding to the receptor, we can consider the chemical reaction:

$$O_1 + R \underset{r_1}{\overset{k_1}{\rightleftharpoons}} O_1R \underset{r_1^*}{\overset{k_1^*}{\rightleftharpoons}} O_1R^*$$

$$O_2 + R \underset{r_2}{\overset{k_2}{\rightleftharpoons}} O_2R \underset{r_2^*}{\overset{k_2^*}{\rightleftharpoons}} O_2R^*$$

$$O_1 + O_2 \underset{a_2}{\overset{a_1}{\rightleftharpoons}} O_1O_2$$

$$O_1O_2 + R \underset{r_{12}}{\overset{k_{12}}{\rightleftharpoons}} O_1O_2R \underset{r_{12}^*}{\overset{k_{12}^*}{\rightleftharpoons}} O_1O_2R^*$$

The solution of the corresponding rate equations at steady state is

$$F(\{c_1, c_2\}) = \frac{F_{max}\left(e_1 \frac{c_1}{EC50_1} + e_2 \frac{c_2}{EC50_2} + e_{12} \frac{ac_1c_2}{EC50_{12}}\right)}{\left(1 + \frac{c_1}{EC50_1} + \frac{c_2}{EC50_2} + \frac{ac_1c_2}{EC50_{12}}\right)}$$

Here $a = a_1/a_2$ is the ratio of the binding and unbinding rates of the odorant molecules. This equation is similar to odorant facilitation. The resulting effects are synergy, overshadowing, suppression and inhibition.

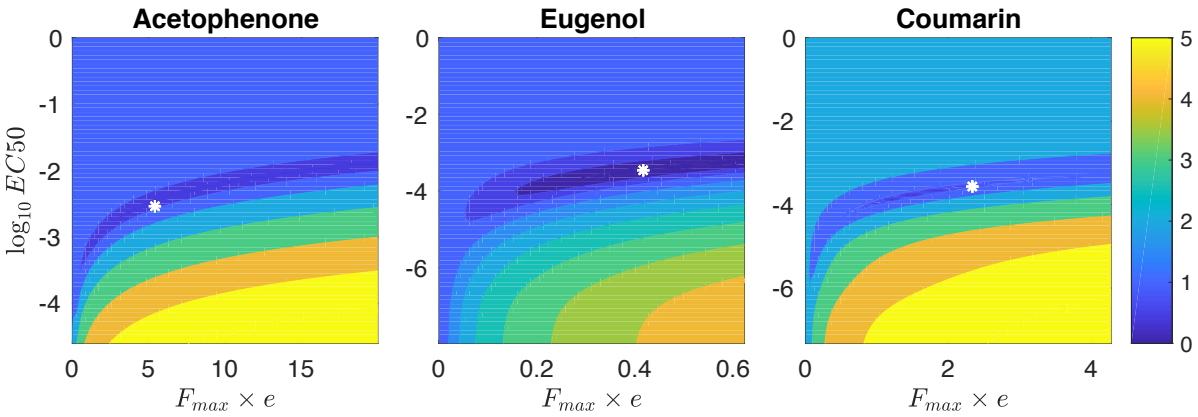

Figure S1: Weighted squared error (see Methods for definition) in fitting the dose-response curves for Olfr895 with different choices of model parameters. The error-minimizing parameters are shown by white markers (*) in each panel. The minimum lies within a long, narrow valley over which the parameters can be widely varied without much change in the error. Thus, most parameters within the valley provide a similar quality fit to the dose-response curves. To reduce the resulting uncertainty in parameters, we fit the competitive binding model to the dose-response data and mixture data simultaneously. This procedure reduces the uncertainty by selecting parameters that are consistent with both the dose-response data and the mixture data.

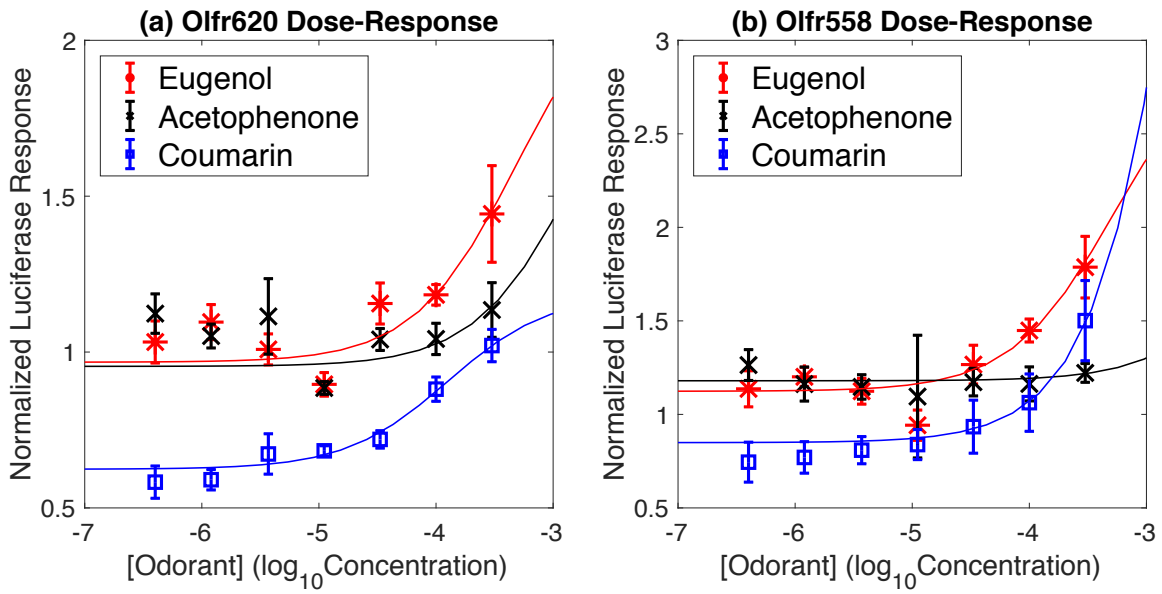

Figure S2: Dose-response curves of Olfr620 and Olfr558 for which the model had large relative error (~70%) in predicting binary-ternary mixture responses. Both receptors show little response to acetophenone compared to baseline. Acetophenone also showed some antagonistic effects in mixture (not shown), where the response to some mixture combinations was lower than the baseline receptor response at zero concentration. The poor performance of the competitive binding model in this case may be because of the difficulty of reliably fitting the weak acetophenone response, along with the absence of antagonism in the model.

SI Table 1: Binary-Ternary Mixture Compositions (concentrations in μM)

	Odorants (μM)		
Mixture #	**Eugenol**	**Acetophenone**	**Coumarin**
1	100	100	0
2	100	0	100
3	0	100	100
4	50	50	0
5	50	0	50
6	0	50	50
7	100	50	0
8	100	0	50
9	50	100	0
10	0	100	50
11	0	50	100
12	50	0	100
13	150	150	150
14	100	100	100
15	50	50	50
16	50	100	150
17	50	150	100
18	100	50	150
18	100	50	150
19	100	150	50
20	150	100	50
21	150	50	100
22	0	0	0

SI Table 2: 12-Component Mixture Compositions (concentrations in μM)

Mixture #	1-Heptanol	2,3-Hexanedione	2-Hexanone	2-Heptanone	3-Heptanone	4-Chromanone	(-)-Carvone	(+)-Carvone	(+)-Dihydrocarvone	Dihydrojasmone	Benzyl acetate	Prenyl acetate
1	100	100	100	100	100	100	100	100	100	100	100	100
2	33	33	33	33	33	33	33	33	33	33	33	33
3	11	11	11	11	11	11	11	11	11	11	11	11
4	3.7	3.7	3.7	3.7	3.7	3.7	3.7	3.7	3.7	3.7	3.7	3.7
5	1.2	1.2	1.2	1.2	1.2	1.2	1.2	1.2	1.2	1.2	1.2	1.2
6	0.4	0.4	0.4	0.4	0.4	0.4	0.4	0.4	0.4	0.4	0.4	0.4
7	3	1	3	1	0.1	1	3	0.1	1	0.1	0.1	1
8	3	1	3	1	1	3	0.1	0.1	3	3	0.1	1
9	0.1	3	1	0.1	3	3	1	1	0.1	0.1	1	1
10	0.1	1	0.1	3	0.1	1	1	1	1	1	3	0.1
11	1	1	3	3	1	3	3	1	10	3	10	1
12	3	1	1	10	10	1	3	1	10	1	10	1
13	10	1	1	1	10	3	3	1	1	10	3	1
14	10	10	10	3	10	30	30	10	3	10	3	3
15	3	3	10	3	30	3	3	30	30	10	3	3
16	10	30	10	3	30	10	10	10	10	10	10	3
17	10	3	10	1	1	3	10	0.1	0.1	1	3	10
18	1	3	10	1	0.1	1	0.1	3	0.1	0.1	3	3
19	1	3	10	3	1	3	0.1	3	1	0.1	1	1
20	0.1	0.1	10	3	10	1	10	0.1	10	1	0.1	10
21	1	0.1	10	1	10	3	1	10	0.1	3	30	1
22	3	30	1	30	0.1	30	1	30	30	0.1	30	1
23	10	30	3	30	0.1	0.1	30	0.1	10	30	0.1	3
24	1	10	1	30	0.1	30	30	0.1	0.1	3	0.1	30
25	0	0	0	0	0	0	0	0	0	0	0	0

SI Table 3: Parameters of The Competitive Binding Model.
(18 receptors used in binary/ternary analysis)

	Eugenol		Acetophenone		Coumarin	
	Fmax*Efficacy	log10(EC50)	Fmax*Efficacy	log10(EC50)	Fmax*Efficacy	log10(EC50)
'OR2W1'	1.034	-4.304	2.494	-3.311	1.878	-3.626
'OR2J2'	0.854	-3.696	0.618	-3.299	1.244	-3.691
'OR5P3'	4.758	-1.872	6.957	-2.687	1.558	-5.184
'OR2C1'	2.887	-2.151	3.980	-1.898	5.553	-2.311
'OR5K1'	0.298	-3.892	5.723	-2.180	1.533	-2.969
'OR1A1'	10.000	-1.841	0.118	-3.183	0.305	-3.154
'OR2J3'	0.965	-3.766	4.345	-2.230	1.498	-3.555
'OR10G4'	0.506	-5.023	0.012	-4.017	0.465	-2.784
'Olfr620'	1.262	-3.317	1.258	-2.777	0.563	-3.902
'Olfr558'	1.885	-3.285	2.065	-1.794	12.431	-2.252
'Olfr429'	0.827	-2.812	5.074	-2.247	0.585	-3.903
'Olfr19'	0.100	-3.448	6.631	-1.867	1.593	-2.124
'Olfr876'	4.599	-1.732	1.505	-3.309	5.727	-2.447
'Olfr895'	0.372	-3.745	7.048	-2.398	2.108	-3.624
'Olfr175-ps1'	1.932	-2.989	2.570	-2.459	0.108	-3.582
'Olfr1062'	6.776	-2.092	1.905	-3.453	1.454	-3.810
'Olfr1079'	0.262	-3.876	0.904	-3.536	4.849	-2.589
'Olfr1104'	0.164	-3.842	0.584	-3.594	1.160	-3.596

SI Table 4: Parameters of The Competitive Binding Model
Two receptors used in 12-component mixture analysis

	OR2W1		Olfr168	
Odorants	Fmax*Efficacy	log10(EC50)	Fmax*Efficacy	log10(EC50)
1-Heptanol	1.452	-4.849	1.287	-3.225
2,3-Hexanedione	0.434	-4.865	0.688	-5.021
2-Hexanone	0.595	-3.980	1.129	-5.302
2-Heptanone	0.811	-4.942	0.807	-5.140
3-Heptanone	0.587	-5.211	0.745	-5.433
4-Chromanone	1.246	-4.086	0.715	-3.830
(-)-Carvone	1.450	-4.577	1.856	-3.844
(+)-Carvone	1.044	-4.745	0.899	-4.164
(+)-Dihydrocarvone	2.165	-4.865	0.847	-3.766
Dihydrojasmone	1.213	-3.843	0.822	-4.273
Benzyl acetate	1.933	-5.374	1.963	-5.364
Prenyl acetate	0.979	-3.968	0.845	-5.506

SI Table 5: List of Odorants Used In The Experiments

Odorant	CAS	SMILE	Catalog Number
(-)-Carvone	6485-40-1	CC1=CCC(CC1=O)C(=C)C	124931-5ML
(+)-Carvone	2244-16-8	CC1=CCC(CC1=O)C(=C)C	22070-25ML
(+)-Dihydrocarvone	5524-05-0	CC1CCC(CC1=O)C(=C)C	37275-25ML
1-Heptanol	111-70-6	CCCCCCCO	H2805-250ML
2,3-Hexanedione	3848-24-6	CCCC(=O)C(=O)C	W255801-SAMPLE-K
2-Heptanone	110-43-0	CCCCCC(=O)C	W254401-SAMPLE-K
2-Hexanone	591-78-6	CCCCC(=O)C	103004-10G
3-Heptanone	106-35-4	CCCCC(=O)CC	W254509-SAMPLE-K
4-Chromanone	491-37-2	C1COC2=CC=CC=C2C1=O	122351-10G
Acetophenone	98-86-2	CC(=O)C1=CC=CC=C1	A10701-100ML
Benzyl acetate	140-11-4	CC(=O)OCC1=CC=CC=C1	B15805-100G
Coumarin	91-64-5	C1=CC=C2C(=C1)C=CC(=O)O2	C4261-50G
Dihydrojasmone	1128-08-1	CCCCCC1=C(CCC1=O)C	W376302-SAMPLE-K
Dimethyl Sulfoxide	67-68-5	CS(=O)C	D8418-100ML
Eugenol	97-53-0	COC1=C(C=CC(=C1)CC=C)O	E51791-100G
Nonanedioic acid	123-99-9	C(CCCC(=O)O)CCCC(=O)O	246379-100G
Prenyl acetate	1191-16-8	CC(=CCOC(=O)C)C	W420201-SAMPLE-K